

Fractional-charge vortex dipoles in spinor Bose-Einstein condensates

Sandeep Gautam^{*1}

¹*Instituto de Física Teórica, Universidade Estadual Paulista - UNESP,
01.140-070 São Paulo, São Paulo, Brazil*

(Dated: March 6, 2022)

We theoretically and numerically investigate the generation of fractional-charge vortex dipoles in spinor condensates with non-zero magnetization. We find that in the antiferromagnetic phase of spin-1 and spin-2 and the cyclic phase of spin-2 condensate with non-zero magnetization coupling of the density (phonon) and a spin-excitation mode results in two critical speeds for vortex-antivortex pair creation in the condensate. As a result, a Gaussian obstacle potential moving across the antiferromagnetic spin-1 or spin-2 and cyclic spin-2 spinor condensates with non-zero magnetization can lead to the creation of fractional-charge vortex dipoles. On the other hand, for zero magnetization, the two modes get decoupled, which is illustrated by a single critical speed for vortex-antivortex pair creation in the condensate due to the phonon excitation mode.

PACS numbers: 03.75.Mn, 03.75.Hh, 03.75.Kk, 67.85.Bc

I. INTRODUCTION

Quantized vortices are the topological excitations of superfluids like Bose-Einstein condensates (BECs) [1]. In contrast to scalar BECs, a wide variety of vortices can exist in spinor BECs [2–4]. In scalar BECs, while traversing a closed loop around the vortex center, the gauge phase of the wave function changes by an integer multiple n of 2π to ensure the single-valuedness of the wave function, where n is the charge of the vortex. The circulation of the velocity field resulting in mass current is quantized to nh/M for these vortices, here M is the mass of an atom [5, 6]. In contrast to this, for the ferromagnetic phases of spin-1 and spin-2 BECs [2, 4] with non-zero spin-expectation per particle, the circulation of the velocity field responsible for the mass current can change continuously by changing spin configurations or spin texture as in the case of coreless vortices [7–10]. In the case of antiferromagnetic phase of spin-1 [11, 12] and spin-2 and cyclic phase of spin-2 BECs [13, 14], the gauge phase of the wave function can change by a fractional multiple n of 2π while traversing a closed loop around the vortex center. This results in the emergence of a fractional-charge vortex with circulation of the velocity field responsible for the mass current equal to a fractional multiple n of h/M , e.g. a half-quantum vortex or Alice vortex in an antiferromagnetic spin-1 BEC [15, 16]. In addition to these vortices, polar-core vortices can also exist in both ferromagnetic and antiferromagnetic phases of spin-1 BECs [8, 9, 17, 18]; these vortices are characterized by component vortices with integer charges ± 1 and 0 in the spin components $m_f = \pm 1$ and 0, respectively [2]. The nucleation of stable fractional-charge vortices in the cyclic spin-2 BEC under rotation has also been theoretically studied [19].

A vortex dipole is a pair of vortices with opposite cir-

ulation and plays crucial roles in the phenomena ranging from superfluid turbulence [20, 21], the Berezinskii-Kosterlitz-Thouless (BKT) phase transition [22–24], and phase transition dynamics via Kibble-Zurek mechanism [25], etc. It has been shown by the numerical simulations that the superfluid flow past an obstacle above a critical velocity becomes dissipative via vortex dipoles generation [26]. According to Landau criterion for the break down of the superfluidity, the critical speed for the dissipation to set in is equal to the minimum phase velocity, i.e. $v_c = \min[\epsilon(p)/p]$, where $\epsilon(p)$ is the energy of an elementary excitation of momentum p [27]. The generation of vortex dipoles by the superfluid flow past an obstacle above a critical speed has been confirmed experimentally [28]. It has also been shown that the critical speed for vortex dipole generation with a penetrable Gaussian obstacle potential is a fraction of the local speed of sound [29].

In this paper, we study the generation of fractional-charge vortex dipoles by a moving Gaussian obstacle potential in a spin-1 antiferromagnetic BEC and spin-2 antiferromagnetic and cyclic BECs with non-zero magnetizations using a set of coupled mean-field Gross-Pitaevskii (GP) equations. We consider spinor BECs in quasi-two-dimensional (quasi-2D) [30] trapping potentials. The minimum energy states of spin-1 and spin-2 BECs with fractional-charge vortex dipoles have only two non-zero component spin states. This allows us to describe the system by a coupled set of two GP equations. We calculate the excitation spectrum and critical speeds of this binary system. We show that coupling of the phonon excitation mode and a spin excitation mode for non-zero magnetization results in two critical speeds for the vortex-antivortex pair (vortex dipole) creation. We exploit this coupling to create fractional-charge vortex dipoles in spinor condensates with non-zero magnetization. In case of spin-1 antiferromagnetic BEC and spin-2 antiferromagnetic and cyclic BECs with zero magnetization, there is a single critical speed for vortex-antivortex pair creation due to the decoupling of the aforementioned two

^{*}sandeepgautam24@gmail.com

modes. The result for flow of an antiferromagnetic spin-1 condensate with zero magnetization across an obstacle are consistent with an earlier study [31].

The paper is organized as follows. In Sec. II, we describe the coupled GP equations for the spin-1 and spin-2 BECs. In Sec. III, we classify different fractional-charge vortex dipoles of spin-1 and spin-2 BECs which we study in this paper. Here, the interaction parameters of the equivalent binary system under rotation are defined in terms of the interaction parameters of the full $(2f + 1)$ -component GP equation. In Sec. IV, we calculate the excitation spectrum of the uniform binary system. The numerical results for the generation fractional-charge vortex dipoles in spin-1 and spin-2 BECs are presented in Sec. V. We conclude the paper by giving a brief summary and discussion in Sec. VI.

II. GP EQUATIONS FOR SPIN-1 AND SPIN-2 BECS

We consider spinor BECs of N atoms of mass M each trapped by quasi-2D traps with $\omega_z \gg \sqrt{\omega_x \omega_y}$, where $\omega_x, \omega_y, \omega_z$ are the confining trap frequencies in x, y, z directions, respectively. In mean-field approximation, such a spin-1 quasi-2D BEC is described by the following set of three coupled two-dimensional GP equations for different spin components $m_f = \pm 1, 0$ [2, 11, 12]

$$\begin{aligned}\mu_{\pm 1}\psi_{\pm 1}(\mathbf{r}) &= \mathcal{H}\psi_{\pm 1}(\mathbf{r}) \pm c_1 F_z \psi_{\pm 1}(\mathbf{r}) + \frac{c_1}{\sqrt{2}} F_{\mp} \psi_0(\mathbf{r}), \\ \mu_0\psi_0(\mathbf{r}) &= \mathcal{H}\psi_0(\mathbf{r}) + \frac{c_1}{\sqrt{2}} [F_- \psi_{-1}(\mathbf{r}) + F_+ \psi_{+1}(\mathbf{r})],\end{aligned}\quad (2)$$

where $\mathbf{F} \equiv \{F_x, F_y, F_z\}$ is a vector whose three components are the expectation values of the three spin-operators over the multicomponent wavefunction, and is called the spin-expectation value [2]. Also,

$$F_{\pm} \equiv F_x \pm iF_y = \sqrt{2}[\psi_{\pm 1}^*(\mathbf{r})\psi_0(\mathbf{r}) + \psi_0^*(\mathbf{r})\psi_{\mp 1}(\mathbf{r})], \quad (3)$$

$$F_z = n_{+1}(\mathbf{r}) - n_{-1}(\mathbf{r}), \quad \mathcal{H} = -\frac{\nabla^2}{2} + V(\mathbf{r}) + c_0 n, \quad (4)$$

$$c_0 = \frac{2N\sqrt{2\pi\gamma}(a_0 + 2a_2)}{3l_0}, \quad c_1 = \frac{2N\sqrt{2\pi\gamma}(a_2 - a_0)}{3l_0}, \quad (5)$$

$$\nabla^2 = \frac{\partial^2}{\partial x^2} + \frac{\partial^2}{\partial y^2}, \quad V(\mathbf{r}) = \frac{x^2 + \beta^2 y^2}{2}, \quad \mathbf{r} \equiv \{x, y\}, \quad (6)$$

where $n_j = |\psi_j(\mathbf{r})|^2$ with $j = \pm 1, 0$ are the component densities, $n = \sum_j n_j$ is the total density, μ_j with $j = \pm 1, 0$ are the respective chemical potentials, a_0 and a_2 are the s -wave scattering lengths in the total spin 0 and 2 channels, respectively, and asterisk denotes complex conjugate. The normalization condition satisfied by the component wavefunctions ψ_j is $\int \sum_j n_j d\mathbf{r} = 1$. Here $l_0 = \sqrt{\hbar/(M\omega_x)}$ is the oscillator length along x axis, $\beta = \omega_y/\omega_x$ and $\gamma = \omega_z/\omega_x$ are anisotropy parameters. Here the units of length, density and chemical potential are l_0, l_0^{-2} , and $\hbar\omega_x$, respectively.

In the same manner, five coupled GP equations, for different spin components $m_f = \pm 2, \pm 1, 0$ of a spin-2 BEC, in dimensionless form are [2, 13]

$$\begin{aligned}\mu_{\pm 2}\psi_{\pm 2}(\mathbf{r}) &= \mathcal{H}\psi_{\pm 2}(\mathbf{r}) + (c_2/\sqrt{5})\Theta\psi_{\mp 2}^*(\mathbf{r}) \\ &+ c_1[F_{\mp}\psi_{\pm 1}(\mathbf{r}) \pm 2F_z\psi_{\pm 2}(\mathbf{r})],\end{aligned}\quad (7)$$

$$\begin{aligned}\mu_{\pm 1}\psi_{\pm 1}(\mathbf{r}) &= \mathcal{H}\psi_{\pm 1}(\mathbf{r}) - (c_2/\sqrt{5})\Theta\psi_{\mp 1}^*(\mathbf{r}) \\ &+ c_1[\sqrt{3/2}F_{\mp}\psi_0(\mathbf{r}) + F_{\pm}\psi_{\pm 2}(\mathbf{r}) \pm F_z\psi_{\pm 1}(\mathbf{r})],\end{aligned}\quad (8)$$

$$\begin{aligned}\mu_0\psi_0(\mathbf{r}) &= \mathcal{H}\psi_0(\mathbf{r}) + (c_2/\sqrt{5})\Theta\psi_0^*(\mathbf{r}) \\ &+ c_1\sqrt{3/2}[F_- \psi_{-1}(\mathbf{r}) + F_+ \psi_{+1}(\mathbf{r})],\end{aligned}\quad (9)$$

where

$$\begin{aligned}F_+ &= F_-^* = 2(\psi_{+2}^*\psi_{+1} + \psi_{-1}^*\psi_{-2}) \\ &+ \sqrt{6}(\psi_{+1}^*\psi_0 + \psi_0^*\psi_{-1}),\end{aligned}\quad (10)$$

$$F_z = 2(n_{+2} - n_{-2}) + n_{+1} - n_{-1}, \quad (11)$$

$$\Theta = \frac{2\psi_{+2}\psi_{-2} - 2\psi_{+1}\psi_{-1} + \psi_0^2}{\sqrt{5}}. \quad (12)$$

Here

$$c_0 = 2N\sqrt{2\pi\gamma}\frac{4a_2 + 3a_4}{7l_0}, \quad (13)$$

$$c_1 = 2N\sqrt{2\pi\gamma}\frac{a_4 - a_2}{7l_0}, \quad (14)$$

$$c_2 = 2N\sqrt{2\pi\gamma}\frac{7a_0 - 10a_2 + 3a_4}{7l_0}, \quad (15)$$

a_0, a_2 , and a_4 are the s -wave scattering lengths in the total spin 0, 2 and 4 channels, respectively, and μ_j with $j = \pm 2, \pm 1, 0$ are the respective chemical potentials. All other variables have the same definitions as in the spin-1 case.

In the absence of magnetic field, depending on the values of the interaction parameters c_j , the ground state phase of the spinor BEC is either ferromagnetic or antiferromagnetic (polar) for spin-1 BEC [11, 12] and is ferromagnetic or antiferromagnetic or cyclic for spin-2 BEC [2, 14].

III. FRACTIONAL-CHARGE VORTEX DIPOLES

The superfluid velocity $\mathbf{v}_s = \hbar\nabla\theta/M$ for a spinor BEC with zero spin expectation value ($\mathbf{F} = 0$), where θ is the gauge phase of the wave function. Hence, antiferromagnetic phase of spin-1, spin-2 and cyclic phase of spin-2 cyclic BECs, each of which have $\mathbf{F} = 0$, are irrotational ($\nabla \times \mathbf{v}_s = \mathbf{0}$), and the circulation of the velocity field is quantized [2], i.e. $\oint \mathbf{v}_s \cdot d\mathbf{l} = nh/M$, where n is an integer or a rational fraction. The vortices with n equal to a rational fraction are known as fractional-charge vortices, which emerge due to the fact that a spinor BEC

has SO(3) rotational symmetry along with U(1) global gauge symmetry of a scalar BEC [2, 32]. In the present manuscript, we consider the rotation only around z axis as the condensate lies in x - y plane with no dynamics along z axis, in which case the antiferromagnetic and cyclic phases of the spinor BEC with non-zero (longitudinal) magnetization ($\mathcal{M} = \int F_z(\mathbf{r})d\mathbf{r} \neq 0$) are also irrotational [2], and the concept of fractional charge can be extended to these phases of spinor condensate with non-zero \mathcal{M} .

A. Spin-1 BEC

There is a single non-degenerate ground state of the spin-1 antiferromagnetic BEC with non-zero \mathcal{M} in contrast to two degenerate ground states with $\mathcal{M} = 0$ [33]. The rotation operator around direction z for the spin-1 BEC is [2]

$$\mathcal{D}(\alpha) = \begin{pmatrix} e^{-i\alpha} & 0 & 0 \\ 0 & 1 & 0 \\ 0 & 0 & e^{i\alpha} \end{pmatrix}. \quad (16)$$

A general normalized state with $\mathcal{M} \neq 0$ can be obtained by operating $\mathcal{D}(\alpha)$ on the state

$$\chi_0 = \left(\sqrt{\frac{1+\mathcal{M}}{2}}, 0, \sqrt{\frac{1-\mathcal{M}}{2}} \right)^T \quad (17)$$

and can be written as

$$\begin{aligned} \chi &= e^{i\theta} \mathcal{D}(\alpha) \chi_0 \\ &= \left[e^{-i(\alpha-\theta)} \sqrt{\frac{1+\mathcal{M}}{2}}, 0, e^{i(\alpha+\theta)} \sqrt{\frac{1-\mathcal{M}}{2}} \right]^T, \end{aligned} \quad (18)$$

where θ is the overall gauge phase. The simplest way to obtain a single-valued spinor with a fractional gauge charge ($\theta \neq 0$) is to consider $\theta = \alpha = \beta/2$ [34], where β is azimuthal angle. The wave function, then, is

$$\chi = \left[\sqrt{\frac{1+\mathcal{M}}{2}}, 0, e^{i\beta} \sqrt{\frac{1-\mathcal{M}}{2}} \right]^T. \quad (19)$$

This is a 1/2-1/2 vortex, i.e. 1/2 unit each of gauge and spin charge, located at origin. In general 1/2-1/2 vortex located at (x_1, y_1) , which may or may not coincide with origin, can be described by wave function

$$\chi = \left[\sqrt{\frac{1+\mathcal{M}}{2}}, 0, e^{i \tan^{-1} \frac{y-y_1}{x-x_1}} \sqrt{\frac{1-\mathcal{M}}{2}} \right]^T. \quad (20)$$

If in addition to the vortex at (x_1, y_1) there is also an antivortex at (x_2, y_2) in component ψ_{-1} , the wavefunction can be written as

$$\chi_{\text{vd}} = \left[\sqrt{\frac{1+\mathcal{M}}{2}}, 0, e^{i(\tan^{-1} \frac{y-y_1}{x-x_1} - \tan^{-1} \frac{y-y_2}{x-x_2})} \sqrt{\frac{1-\mathcal{M}}{2}} \right]^T, \quad (21)$$

which is wavefunction for spin-1 condensate with a half-quantum vortex dipole.

B. Spin-2 BEC

Antiferromagnetic: There is a single non-degenerate ground state of a non-rotating spin-2 antiferromagnetic BEC with non-zero magnetization [33]. The rotation operator around z direction for spin-2 BEC is [2]

$$\mathcal{D}(\alpha) = \begin{pmatrix} e^{-2i\alpha} & 0 & 0 & 0 & 0 \\ 0 & e^{-i\alpha} & 0 & 0 & 0 \\ 0 & 0 & 1 & 0 & 0 \\ 0 & 0 & 0 & e^{i\alpha} & 0 \\ 0 & 0 & 0 & 0 & e^{2i\alpha} \end{pmatrix}. \quad (22)$$

One can obtain a general normalized wave function by operating $\mathcal{D}(\alpha)$ on the representative state

$$\chi_0 = \left[\frac{\sqrt{2+\mathcal{M}}}{2}, 0, 0, 0, \frac{\sqrt{2-\mathcal{M}}}{2} \right]^T \quad (23)$$

and is given as

$$\chi = e^{i\theta} \left[e^{-2i\alpha} \frac{\sqrt{2+\mathcal{M}}}{2}, 0, 0, 0, e^{2i\alpha} \frac{\sqrt{2-\mathcal{M}}}{2} \right]^T. \quad (24)$$

The single-valuedness of the wave function with a fractional-charge vortex can be preserved by considering $\theta = \beta/2, \alpha = \beta/4$ to get

$$\chi = \left[\frac{\sqrt{2+\mathcal{M}}}{2}, 0, 0, 0, e^{i\beta} \frac{\sqrt{2-\mathcal{M}}}{2} \right]^T, \quad (25)$$

which is a 1/2-1/4 vortex or a half-quantum vortex. Again, as in the case spin-1 condensate, replacing $\beta = \tan^{-1} \frac{y-y_1}{x-x_1} - \tan^{-1} \frac{y-y_2}{x-x_2}$, the aforementioned wavefunction describes a 1/2,1/4 vortex dipole.

Cyclic: There are two degenerate ground states of a non-rotating spin-2 cyclic BEC for any arbitrary value of \mathcal{M} [33], and only one of them with $\psi_{+1} = \psi_0 = \psi_{-2} = 0$ leads to fractional-charge vortex states. Thus, a general normalized wave function under rotation can be written as [34]

$$\chi = e^{i\theta} \left[e^{-2i\alpha} \sqrt{\frac{1+\mathcal{M}}{3}}, 0, 0, e^{i\alpha} \sqrt{\frac{2-\mathcal{M}}{3}}, 0 \right]^T. \quad (26)$$

There are four simple ways to maintain a single-valued spinor function to generate a fractional-charge vortex [19]:

$$\theta = \beta/3, \alpha = 2\beta/3, \quad (27)$$

$$\theta = -\beta/3, \alpha = \beta/3, \quad (28)$$

$$\theta = -2\beta/3, \alpha = 2\beta/3 \quad (29)$$

$$\theta = 2\beta/3, \alpha = \beta/3. \quad (30)$$

Replacing β by $\tan^{-1} \frac{y-y_1}{x-x_1} - \tan^{-1} \frac{y-y_2}{x-x_2}$ in Eqs. (27)-(30) and then substituting in Eq. (26), one can obtain the wavefunctions describing 1/3- and 2/3-quantum vortex dipoles in cyclic spin-2 condensate.

In all the cases discussed above of fractional-charge vortex dipoles, the spinor BEC has all but two of the component wavefunctions zero. Thus, the GP equations for the spinor BEC simplify to that for a two-component BEC [34] and can be written as [34]

$$i \frac{\partial}{\partial t} \phi_j = \left[-\frac{\nabla^2}{2} + \frac{x^2 + y^2}{2} + g_j \phi_j^2 + g_{12} \phi_{3-j}^2 \right] \phi_j, \quad (31)$$

$$\nabla^2 = \frac{\partial}{\partial x^2} + \frac{\partial}{\partial y^2}, \quad (32)$$

where $j = 1, 2$, g_j and g_{12} are the intra-component and inter-component interaction parameters, respectively. For antiferromagnetic phase of spin-1 and spin-2 BEC with a half-quantum vortex dipole and coupling the two non-zero components, these interaction parameters are

$$g_1 = g_2 = c_0 + c_1, \quad g_{12} = c_0 - c_1. \quad (33)$$

$$g_1 = g_2 = c_0 + 4c_1, \quad g_{12} = c_0 - 4c_1 + 2c_2/5, \quad (34)$$

respectively [34]. Similarly, for a spin-2 cyclic BEC with a fractional-charge vortex dipole and coupling $\psi_{+2} = \phi_1$ and $\psi_{-1} = \phi_2$, the interaction parameters are [34]

$$g_1 = c_0 + 4c_1, \quad g_2 = c_0 + c_1, \quad g_{12} = c_0 - 2c_1. \quad (35)$$

Eqs. (33)-(35) are the definitions of intra- and inter-species interaction parameters of a two-component BEC which can be treated as equivalent to a spinor BEC hosting a fractional-charge vortex dipole.

IV. CRITICAL SPEEDS FOR THE BINARY SYSTEM

The critical speed for vortex shedding v_c in compressible fluid by a penetrable obstacle is a fraction of the local speed of sound [29, 35]. Hence, in order to understand the emergence of two different critical speeds for vortex dipole shedding in antiferromagnetic and cyclic phases of spinor condensate, we calculate the excitation spectrum of the uniform binary system, introduced in the previous section, representing the spinor BEC. It must be stated that there are a few spin-wave excitations which are not captured by the analysis based on the binary system, but they do not play any role in the vortex shedding dynamics considered in this paper and are decoupled from the modes captured by binary system approach [36]. If $\delta\phi_j$ are the changes in the wavefunctions from their respective unperturbed values, one can derive the Bogoliubov-de Gennes (BdG) equations for the uniform binary condensate ($V = 0$) by linearizing Eqs. (31) around the unperturbed wavefunctions, i.e., substituting $\phi_j = \bar{\phi}_j + \delta\phi_j$ and retaining terms only upto first order in $\delta\phi_j$, we get

$$i \frac{\partial \delta\phi_j}{\partial t} = -\frac{\nabla^2}{2} \delta\phi_j + g_j (2|\bar{\phi}_j|^2 \delta\phi_j + \bar{\phi}_j^2 \delta\phi_j^*) + g_{12} \times (|\bar{\phi}_{3-j}|^2 \delta\phi_j + \bar{\phi}_j \bar{\phi}_{3-j} \delta\phi_{3-j}^* + \bar{\phi}_j \bar{\phi}_{3-j}^* \delta\phi_{3-j}) \quad (36)$$

where $\bar{\phi}_j$ are to be understood as equilibrium values of wavefunctions. Now, we substitute $\phi_j = \sqrt{n_j} e^{-i\mu_j t}$ and $\delta\phi_j = e^{-i\mu_j t} [u_j(\mathbf{r}) e^{-i\omega t} - v_j^*(\mathbf{r}) e^{i\omega t}]$ with $u_j(\mathbf{r})$ and $v_j(\mathbf{r})$ denoting the quasi-particle amplitudes, Eqs. (36) then become

$$(\mu_j + \omega) u_j e^{-i\omega t} - (\mu_j - \omega) v_j^* e^{i\omega t} = -\frac{\nabla^2}{2} (u_j e^{-i\omega t} - v_j^* e^{i\omega t}) + g_j [2n_j (u_j e^{-i\omega t} - v_j^* e^{i\omega t}) + n_j (u_j^* e^{i\omega t} - v_j e^{-i\omega t})] + g_{12} [n_{3-j} (u_j e^{-i\omega t} - v_j^* e^{i\omega t}) + \sqrt{n_1 n_2} (u_{3-j}^* e^{i\omega t} - v_{3-j} e^{-i\omega t} + u_{3-j} e^{-i\omega t} - v_{3-j}^* e^{i\omega t})], \quad (37)$$

Finally, we equate the coefficients of $e^{\mp i\omega t}$ on both sides of Eqs. (37). The coupled BdG equations thus obtained are

$$A(u_1, v_1, u_2, v_2)^T = \omega(u_1, v_1, u_2, v_2)^T, \quad (38)$$

where A is a 4×4 matrix whose elements for a uniform system are given as [37]

$$\begin{aligned} A_{11} &= -\frac{\nabla^2}{2} + 2g_1 n_1 + g_{12} n_2 - \mu_1, \quad A_{12} = -g_1 n_1 \\ A_{13} &= g_{12} \sqrt{n_1 n_2}, \quad A_{14} = -g_{12} \sqrt{n_1 n_2} \\ A_{21} &= g_1 n_1, \quad A_{22} = -\left(-\frac{\nabla^2}{2} + 2g_1 n_1 + g_{12} n_2\right) + \mu_1 \\ A_{23} &= g_{12} \sqrt{n_1 n_2}, \quad A_{24} = -g_{12} \sqrt{n_1 n_2} \\ A_{31} &= g_{12} \sqrt{n_1 n_2}, \quad A_{32} = -g_{12} \sqrt{n_1 n_2} \\ A_{33} &= -\frac{\nabla^2}{2} + 2g_2 n_2 + g_{12} n_1 - \mu_2, \quad A_{34} = -g_2 n_2 \\ A_{41} &= g_{12} \sqrt{n_1 n_2}, \quad A_{42} = -g_{12} \sqrt{n_1 n_2} \\ A_{43} &= g_2 n_2, \quad A_{44} = -\left(-\frac{\nabla^2}{2} + 2g_2 n_2 + g_{12} n_1\right) + \mu_2. \end{aligned}$$

For a uniform system with $\mu_1 = g_1 n_1 + g_{12} n_2$ and $\mu_2 = g_2 n_2 + g_{12} n_1$, seeking solutions of form $u(\mathbf{r}) = u_q e^{i\mathbf{q}\cdot\mathbf{r}}/\sqrt{\mathcal{V}}$ and $v(\mathbf{r}) = v_q e^{i\mathbf{q}\cdot\mathbf{r}}/\sqrt{\mathcal{V}}$ where \mathcal{V} is the volume (area) in

three (two)-dimensional space, the excitation spectrum for the consistent solutions of BdG equations is

$$\omega_{\pm} = \frac{q}{2} \sqrt{2g_1 n_1 + 2g_2 n_2 \pm 2\sqrt{(g_1^2 n_1^2 - 2g_1 g_2 n_1 n_2 + 4g_{12}^2 n_1 n_2 + g_2^2 n_2^2)} + q^2}. \quad (39)$$

For spin-1 antiferromagnetic condensate, using $n_1 = (1 + \mathcal{M})n/2$, $n_2 = (1 - \mathcal{M})n/2$ where n is the total density of

the uniform system, and Eq. (33) in Eq. (39), we get

$$\omega_{\pm} = \frac{q \sqrt{2c_0 n + 2c_1 n \pm 2n \sqrt{c_0^2 - 2c_0 c_1 + c_1^2 + 4c_0 c_1 \mathcal{M}^2} + q^2}}{2}. \quad (40)$$

It has been shown in Ref. [2] that these two excitations are coupled and correspond to coupled phonon and magnon excitations, with two critical speeds

$$c_{\pm} = \lim_{q \rightarrow 0} \frac{\omega_{\pm}(q)}{q}, \quad (41)$$

$$= \frac{\sqrt{2c_0 n + 2c_1 n \pm 2n \sqrt{c_0^2 - 2c_0 c_1 + c_1^2 + 4c_0 c_1 \mathcal{M}^2}}}{2} \quad (42)$$

Depending upon whether \mathcal{M} is zero or not zero, the two critical speeds can lead to single, v_c , or two different, v_c^l and v_c^h , critical speeds for vortex dipole shedding by a moving obstacle potential. If $\mathcal{M} = 0$, the two modes become decoupled with excitation frequency given by

$$\omega_+ = \frac{q \sqrt{4c_0 n + q^2}}{2}, \quad (43)$$

$$\omega_- = \frac{q \sqrt{4c_1 n + q^2}}{2}, \quad (44)$$

with two critical speeds

$$c_+ = \sqrt{c_0 n} \quad (45)$$

$$c_- = \sqrt{c_1 n}. \quad (46)$$

The decoupling of the critical speeds for phonon c_+ and magnon c_- excitations at $\mathcal{M} = 0$ results in a single critical speed v_c for the vortex-antivortex nucleation by a moving obstacle and corresponds to critical speed for phonon excitation which can lead to density fluctuations. As mentioned earlier, for a penetrable obstacle potential v_c should be the fraction of c_+ . In this case, the critical speed for spin excitations c_- is not associated with the vortex shedding phenomenon. On the other hand, coupling of the two modes for $\mathcal{M} \neq 0$ results in two critical speeds, v_c^l and v_c^h with $v_c^l < v_c^h$, for the vortex-antivortex nucleation by a moving obstacle. This coupling of the modes can be used to create half-quantum vortex dipole in spin-1 antiferromagnetic condensate. Again v_c^l and v_c^h are fractions of c_- and c_+ , respectively. Similarly, the two critical speeds for antiferromagnetic and cyclic spin-2 condensate are, respectively,

$$c_{\pm} = \frac{\sqrt{10c_0 n + 40c_1 n \pm 2n \sqrt{25c_0^2 + 400c_1^2 - 20c_1 c_2 (4 - \mathcal{M}^2) + c_2^2 (4 - \mathcal{M}^2) + 5c_0 (c_2 (4 - \mathcal{M}^2) + 20c_1 (\mathcal{M}^2 - 2))}}}{2\sqrt{5}} \quad (47)$$

$$c_{\pm} = \frac{\sqrt{2c_0 n + 4c_1 n + 2c_1 n \mathcal{M} \pm 2n \sqrt{c_0^2 + c_1^2 (2 + \mathcal{M})^2 + 2c_0 c_1 (2\mathcal{M}^2 - \mathcal{M} - 2)}}}{2}. \quad (48)$$

As in case of antiferromagnetic spin-1 condensate, the phonon and spin modes gets decoupled for $\mathcal{M} = 0$, re-

sulting in single critical speed for vortex-antivortex pair

creation by a moving obstacle.

V. NUMERICAL RESULTS

We use the time-splitting Fourier pseudo-spectral method to solve the full GP equations for spin-1 and spin-2 condensate [38]. The method automatically implements the periodic boundary conditions used to simulate the uniform system. Alternatively, one can also implement the time-splitting Crank-Nicolson method with explicit periodic boundary conditions to simulate uniform system and box boundary conditions to simulate trapped condensates [39]. We use the imaginary time propagation to obtain the ground state solution and real time propagation to study the dynamics of fractional-charge vortex dipole generation. The space and time steps employed in our study are 0.1 and 0.0005, respectively. We consider spin-1 and spin-2 condensates each of ^{23}Na atoms for numerical simulations. The two scattering lengths of spin-1 ^{23}Na condensate are $a_0 = 47.36a_B$ and $a_2 = 52.98a_B$ [2], and the three scattering lengths of spin-2 condensate of ^{23}Na atoms are $a_0 = 34.9a_B$, $a_2 = 45.8a_B$, and $a_4 = 64.5a_B$ [14], where a_B is Bohr radius. The ground state phases of both spin-1 and spin-2 ^{23}Na condensate with these scattering length values are antiferromagnetic. In order to access the cyclic phase of spin-2 condensate, we reduce a_2 to half of its actual value which can be achieved experimentally by exploiting Feshbach resonances [40]. We consider both the uniform and trapped spinor condensates in our simulations.

Uniform system: We first consider spin-1 antiferromagnetic condensate over a square of size 25.5×25.5 with $c_0 = 6466.5$ and $c_1 = 237.0$. The values of nonlinearities correspond to choosing $N = 50000$, $l_0 = 4.69\mu\text{m}$ (unit of length for numerical simulations), $\gamma = 20$, $a_0 = 47.36a_B$, and $a_2 = 52.98a_B$ in Eqs. (5). We move the Gaussian obstacle potential $V_{\text{obs}} = V_0 e^{-2[(x-x_0(t))^2 + y^2]/w^2}$, initially located at $x_0(0) = -8.0$, with a constant speed v such that $x_0(t) = x_0(0) + vt$, where V_0 and w are the strength and width of the obstacle potential. In spin-1 condensate, we consider $V_0 = 100$ (in dimensionless units), $w_0 = 10\mu\text{m}$. The obstacle is moved with a speed of 0.6 mms^{-1} across the condensate with $\mathcal{M} = 0.5$. We find that a vortex dipole is created in both the components as is shown in Fig. 1, which corresponds to a gauge vortex dipole in scalar condensates. One unit of length in this and other figures in this paper is equal to $4.69\mu\text{m}$. This indicates (almost) same critical speed for vortex-antivortex pair creation in this case. This is due to the fact that in this case $g_{12} = c_0 - c_1 \approx g_1 = g_2$ which results in a single non-zero critical speed c_+ from Eq. (39). The critical speed for vortex dipole shedding obtained from the numerical simulations is $v_c \approx 0.59 \text{ mms}^{-1}$ which is a fraction (0.32 times) of the speed of the "sound" $c_+ \simeq 1.86 \text{ mms}^{-1}$ obtained from Eq. (42). This is in good agreement with the estimation for the critical speed in compressible superfluids [29, 35, 41].

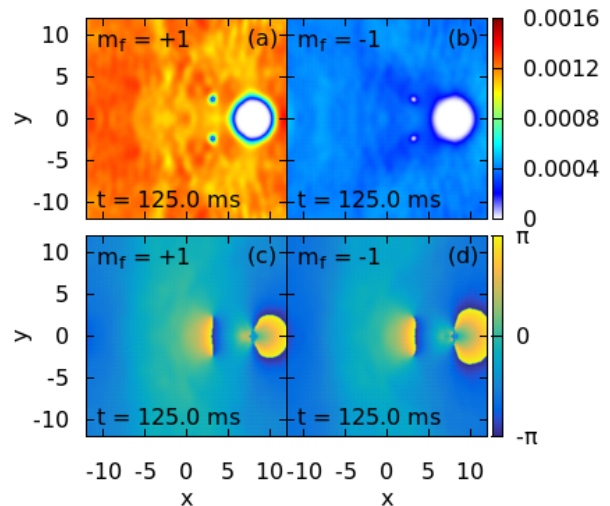


FIG. 1: (Color online) Nucleation of a gauge vortex dipole in uniform antiferromagnetic spin-1 condensate of ^{23}Na with $c_0 = 6466.5$, $c_1 = 237.0$, and $\mathcal{M} = 0.5$. (a)-(b) and (c)-(d) show the density and phase plots, respectively. All the variables in this and the other figures in this paper are in dimensionless units.

In order to confirm the coupling between the phonon and magnon modes, we consider antiferromagnetic spin-1 condensate with $c_0 = 8701.0$ and $c_1 = 1354.3$ over a box of size 25.5×25.5 . The values of nonlinearities correspond to choosing $N = 50000$, $l_0 = 4.69\mu\text{m}$, $\gamma = 20$, $a_0 = 47.36a_B$, and $a_2 = 79.47a_B$ in Eqs. (5). In this case, moving the same obstacle potential at a speed of 0.5 mms^{-1} across the condensate with $\mathcal{M} = 0.5$ leads to the shedding of vortex dipole in $m_f = -1$ component which is $1/2, 1/2$ vortex dipole as is shown in Fig. 2. Numerically, we find that there are two critical speeds $v_c^l \approx 0.37 \text{ mms}^{-1}$ and $v_c^h \approx 0.63 \text{ mms}^{-1}$ for vortex dipole shedding in this case, and 0.5 mms^{-1} is greater than the smaller of the two. When moved with a speed greater than 0.63 mms^{-1} , $1/2, 1/2$ vortex dipoles with singularities in $m_f = 1$ component are also created. The two critical speeds are fractions of the two speeds of "sound", $\simeq 0.715 \text{ mms}^{-1}$ and $\simeq 2.185 \text{ mms}^{-1}$ obtained from Eq. (42). The size of the vortex in a condensate is of the order of coherence length, which for a binary condensate is $\xi_j = 1/\sqrt{2(g_j n_j + g_{12} n_{3-j})} = 1/\sqrt{2}\mu_j$, where n_j and n_{3-j} are the uniform component densities. Using this relation, the size of the vortex cores is 0.2 in this case.

In the case of antiferromagnetic spin-2 condensate, we consider $c_0 = 6809.1$, $c_1 = 338.0$, $c_2 = -365.1$ over a square of size 25.5×25.5 . The values of nonlinearities correspond to choosing $N = 50000$, $l_0 = 4.69\mu\text{m}$, $\gamma = 20$, $a_0 = 34.9a_B$, $a_2 = 45.8a_B$, $a_4 = 64.5$ in Eqs. (13-15). Similarly, for the cyclic spin-2 condensate, we consider $c_0 = 5153.4$, $c_1 = 751.9$, $c_2 = 3774.2$, which correspond to choosing $N = 50000$, $l_0 = 4.69\mu\text{m}$, $\gamma = 20$, $a_0 = 34.9a_B$, $a_2 = 27.9a_B$, $a_4 = 64.5$ in Eqs. (13-15).

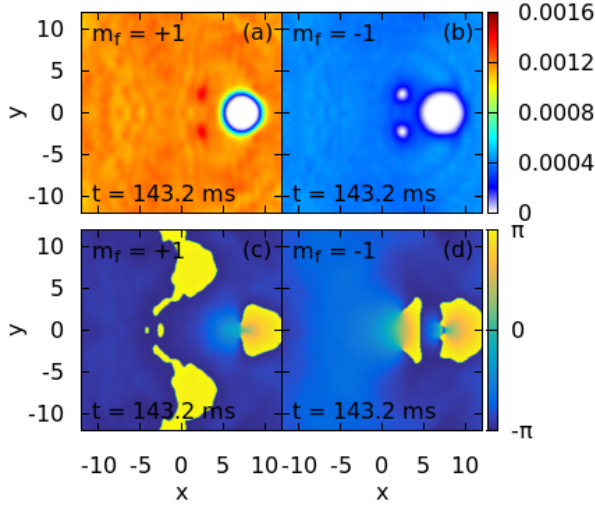


FIG. 2: (Color online) Nucleation of a $1/2, 1/2$ fractional vortex dipole in uniform antiferromagnetic spin-1 condensate of ^{23}Na with $c_0 = 8701.0$, $c_1 = 1354.3$, and $\mathcal{M} = 0.5$. (a)-(b) and (c)-(d) show the density and phase plots, respectively.

For both the antiferromagnetic and cyclic phases, we consider $V_0 = 50$ and $w_0 = 10\mu\text{m}$. Here moving the obstacle potential with a speed of 0.525 mms^{-1} across the condensate with $\mathcal{M} = 0.5$ leads to the creation of $1/2, 1/4$ and $2/3, 1/3$ vortex dipoles in the antiferromagnetic and cyclic phases respectively; these are shown in Fig. 3 and Fig. 4, respectively. The coherence lengths as a measure

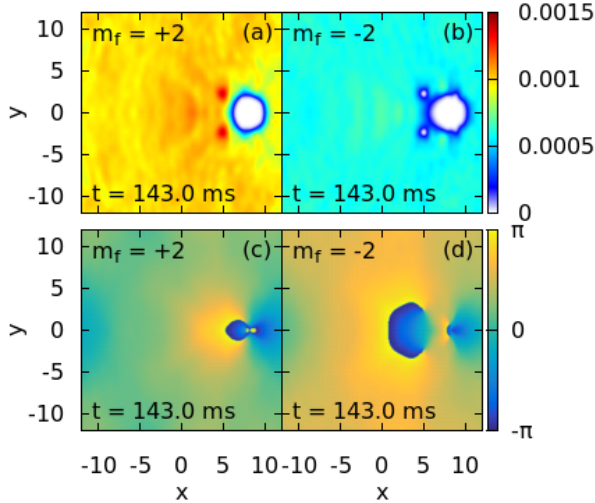


FIG. 3: (Color online) Nucleation of a $1/2, 1/4$ fractional vortex dipole in uniform antiferromagnetic spinor condensate of ^{23}Na with $c_0 = 6809.1$, $c_1 = 338.0$, $c_2 = -365.1$, and $\mathcal{M} = 0.5$. (a)-(b) and (c)-(d) show the density and phase plots, respectively.

of the size of the vortex cores are 0.23 and 0.26 for the

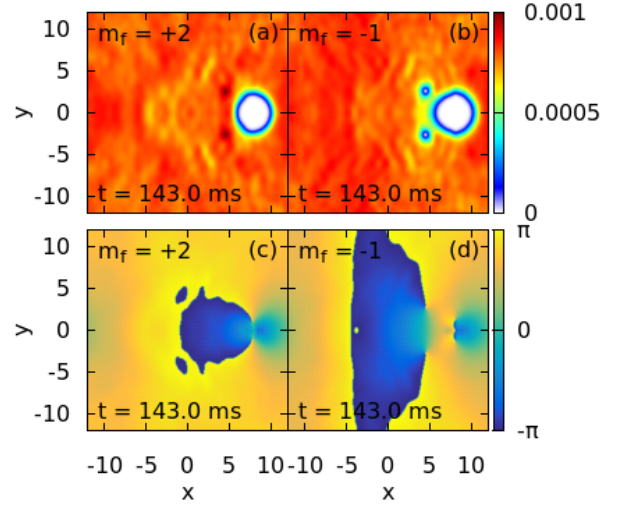


FIG. 4: (Color online) Nucleation of a $2/3, 1/3$ fractional vortex dipole in uniform cyclic spinor condensate of ^{23}Na with $c_0 = 5153.4$, $c_1 = 751.9$, $c_2 = 3774.2$, and $\mathcal{M} = 0.5$. (a)-(b) and (c)-(d) show the density and phase plots, respectively.

antiferromagnetic and cyclic phases, respectively.

Trapped system: To illustrate the creation of fractional-charge vortex dipoles in trapped systems, we consider 5×10^4 spin-2 ^{23}Na atoms trapped in quasi-2D trap with $\omega_x = \omega_y = 2\pi \times 20$, $\omega_z = 2\pi \times 400$ along with a Gaussian obstacle potential V_{obs} initially located at $x_0(0) = 0$. The oscillator length $l_0 = 4.69\mu\text{m}$ with these set of parameters. Here while moving the obstacle potential along x axis with a constant speed, its strength is continuously decreased at a constant rate in order to make V_{obs} vanish at some desired point on the x axis. We consider $V_0 = 100\hbar\omega_x$ as the initial strength of the obstacle potential. The obstacle is moved along x axis with a speed of 0.6 mms^{-1} . The obstacle traverses a distance of $5a_{\text{osc}}$ before it vanishes. The generation of a single $2/3, 1/3$ fractional vortex dipole in the cyclic phase with $\mathcal{M} = 0.5$ is shown in Fig. 5. Similarly, we were able to generate half-quantum vortices in the antiferromagnetic phases of spin-1 and spin-2 condensates of 50000 ^{23}Na atoms each with $\mathcal{M} = 0.5$ and scattering length values same as in Figs. 2 and 3.

In both the antiferromagnetic and cyclic phases, reducing the \mathcal{M} to zero leads to the generation of gauge vortex dipoles as is shown in Figs. 6 (b) and (e) for the cyclic phase. This is consistent with fact that the phonon excitation mode gets decoupled from the spin excitation mode as discussed in the previous section, which results in a single critical speed for vortex-antivortex pair creation in the system. Interestingly, the gauge vortices, shown in Figs. 6 (b) and (e), later on decay into a pair of $1/3$ and $2/3$ fractional-charge vortices as is shown in Figs. 6 (c) and (f). This dynamical instability of the gauge vortices is consistent with a recent experiment where the

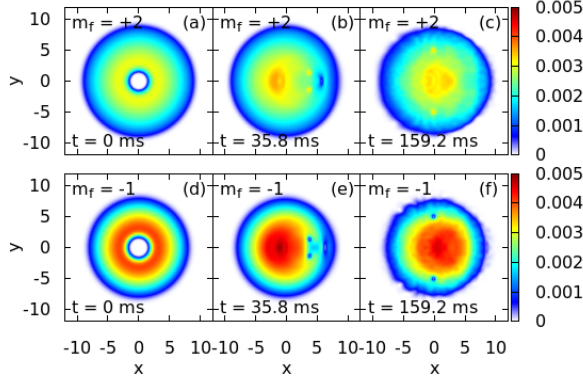


FIG. 5: (Color online) Creation of $2/3, 1/3$ vortex dipole in a cyclic spinor condensate of 50000 ^{23}Na atoms with $a_0 = 34.9a_B$, $a_2 = 27.9a_B$, $a_4 = 64.5a_B$, and $\mathcal{M} = 0.5$.

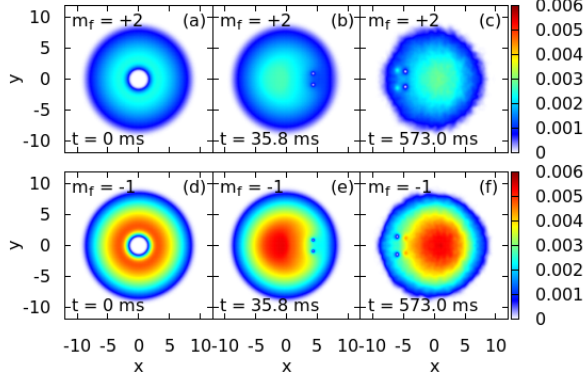


FIG. 6: (Color online) Creation of $1/3, 1/3$ (dipole in component $m_f = +2$) and $2/3, 1/3$ (dipole in component $m_f = -1$) vortex dipoles in a cyclic spin-2 condensate of 50000 ^{23}Na atoms with $a_0 = 34.9a_B$, $a_2 = 27.9a_B$, $a_4 = 64.5a_B$, and $\mathcal{M} = 0$. (a) and (d), (b) and (e), and (c) and (f) show, respectively, the initial density profiles, the density profiles with a gauge vortex dipole in each component, and the density profiles with a $1/3$ - and $2/3$ -quantum vortex dipoles.

decay of a gauge vortex into two half-quantum vortices in an antiferromagnetic spin-1 condensate was observed [16], and is due to the fact that a gauge vortex is energetically unstable to decay into two half-quantum vortices in the antiferromagnetic spin-1 condensate [42]. We find that in some cases a small perturbation, like a small non-zero magnetization, is needed to initiate the decay of the gauge vortex dipole into a pair of fractional-charge vortices. For example, the generation of a pair of $1/2, 1/4$ vortex dipoles created in the antiferromagnetic phase of the spin-2 ^{23}Na condensate with $\mathcal{M} = 0.005$ is shown in Fig. 7. In this case, we introduced a small difference in the population of the atoms in $m_f = +2$ and $m_f = -2$ sublevels to initiate the decay of the gauge vortices, shown in Figs. 7(b) and (e), into a pair of $1/2, 1/4$

vortices shown in Figs. 7(c) and (f).

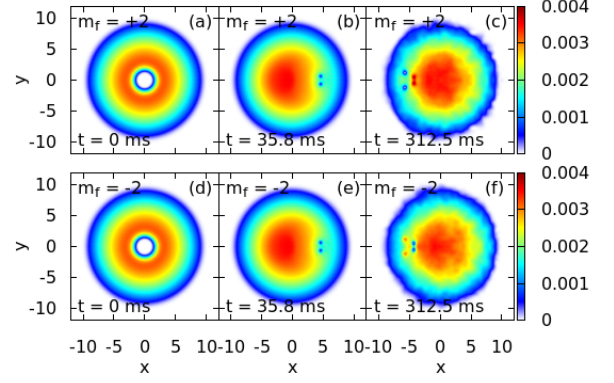


FIG. 7: (Color online) Nucleation of $1/2, 1/4$ vortex dipoles, two pairs, in an antiferromagnetic spin-2 condensate of 50000 ^{23}Na atoms with $a_0 = 34.9a_B$, $a_2 = 45.8a_B$, $a_4 = 64.5a_B$ and $\mathcal{M} = 0.005$. (a) and (d), (b) and (e), and (c) and (f) show, respectively, the initial density profiles, the density profiles with a gauge vortex dipole in each component, and the density profiles with a $1/2, 1/4$ vortex dipole in each component.

VI. SUMMARY AND DISCUSSION

We show that the coupling of the phonon excitation mode and a spin excitation mode in antiferromagnetic phase of spin-1 and antiferromagnetic and cyclic phases of spin-2 condensates with non-zero magnetization results in two critical velocities for vortex dipole shedding in these systems. When an obstacle potential is moved with a velocity which is in between these two velocities, vortex dipoles are shed only in one of the components of the spinor condensate. These vortex dipoles with phase singularities appearing in only one of two non-zero components of the spinor condensate are vortex dipoles with fractional charge. The coupling is absent in antiferromagnetic and cyclic phases with zero magnetization resulting in a single critical speed for vortex dipole shedding and is a fraction of the critical speed for phonon excitation mode. Here, moving the obstacle potential initially generates vortex dipoles in both the components, also the phase singularities corresponding to vortex dipole in one component coincide with the phase-singularities in the other non-zero component. These are usual gauge vortex dipoles investigated earlier in antiferromagnetic spin-1 condensate [31]. We find that a small perturbation like a very small non-zero magnetization can lead to the decay of the an initially formed gauge vortex dipole into two fractional-charge vortex dipoles. This can have implications in future experiments on these systems since notwithstanding the fact that the global minima in energies of antiferromagnetic and cyclic phases of the spinor condensates occurs for zero magnetization, the condensates prepared in experiments will invariably

have some remnant non-zero magnetization which remains conserved over the life time of the condensate [2].

Acknowledgments

This work is financed by FAPESP (Brazil) under Contract No. 2013/07213-0. I thank Prof. S. K. Adhikari for

useful discussions.

-
- [1] R. J. Donnelly, *Quantized Vortices in Helium II* (Cambridge University Press, Cambridge, UK, 1991).
 - [2] Y. Kawaguchi and M. Ueda, *Phys. Rep.* **520**, 253 (2012).
 - [3] D. M. Stamper-Kurn and M. Ueda, *Rev. Mod. Phys.* **85**, 1191 (2013).
 - [4] M. Ueda, *Rep. Prog. Phys.* **77**, 122401 (2014).
 - [5] L. Onsager, *Nuovo Cimento Suppl.* **6**, 249 (1949); R. P. Feynman, *Prog. Low Temp. Phys.* **1**, 17 (1955).
 - [6] A. L. Fetter, *Rev. Mod. Phys.* **81**, 647 (2009).
 - [7] T. Mizushima, K. Machida, and T. Kita, *Phys. Rev. Lett.* **89**, 030401 (2002).
 - [8] T. Mizushima, K. Machida, and T. Kita, *Phys. Rev. A* **66**, 053610 (2002).
 - [9] T. Mizushima, N. Kobayashi, and K. Machida, *Phys. Rev. A* **70**, 043613 (2004).
 - [10] A. E. Leanhardt, Y. Shin, D. Kielpinski, D. E. Pritchard, and W. Ketterle, *Phys. Rev. Lett.* **90**, 140403 (2003).
 - [11] T. Ohmi, K. Machida, *J. Phys. Soc. Japan* **67**, 1822 (1998).
 - [12] T.-L. Ho, *Phys. Rev. Lett.* **81**, 742 (1998).
 - [13] M. Koashi and M. Ueda, *Phys. Rev. Lett.* **84**, 1066 (2000); M. Ueda and M. Koashi, *Phys. Rev. A* **65**, 063602 (2002).
 - [14] C. V. Ciobanu, S.-K. Yip, and T.-L. Ho, *Phys. Rev. A* **61**, 033607 (2000).
 - [15] F. Zhou, *Int. J. Mod. Phys. B* **17**, 2643 (2003); U. Leonhardt and G.E. Volovik, *JETP Lett.* **72**, 46 (2000); A.-C. Ji, W. M. Liu, J. L. Song, and F. Zhou, *Phys. Rev. Lett.* **101**, 010402 (2008).
 - [16] S. W. Seo, S. Kang, W. J. Kwon, and Y.-il Shin, *Phys. Rev. Lett.* **115**, 015301 (2015).
 - [17] T. Isoshima, K. Machida, and T. Ohmi, *J. Phys. Soc. Japan* **70**, 1604 (2001); T. Isoshima and K. Machida, *Phys. Rev. A* **66**, 023602 (2002).
 - [18] L. E. Sadler, J. M. Higbie, S. R. Leslie, M. Vengalattore and D. M. Stamper-Kurn, *Nature (London)* **443**, 312 (2006).
 - [19] J. A. M. Huhtamäki, T. P. Simula, M. Kobayashi, and K. Machida, *Phys. Rev. A* **80**, 051601(R) (2009).
 - [20] M. Kobayashi and M. Tsubota, *Phys. Rev. Lett.* **94**, 065302 (2002); T.-L. Horng, C.-H. Hsueh, and S.-C. Gou, *Phys. Rev. A* **77**, 063625 (2008); M. Tsubota, M. Kobayashi, and H. Takeuchi, *Phys. Rep.* **522**, 191 (2013).
 - [21] A. C. White, B. P. Anderson, and V. S. Bagnato, *Proc. Natl. Acad. Sci. USA* **111**, 4719 (2014).
 - [22] V. L. Berezinskii, *Sov. Phys. JETP* **34**, 610 (1972).
 - [23] J. M. Kosterlitz and D. J. Thouless, *J. Phys. C* **6**, 1181 (1973); J. M. Kosterlitz, *ibid.* **7**, 1046 (1974).
 - [24] Z. Hadzibabic, P. Krüger, M. Cheneau, B. Battelier, and J. Dalibard, *Nature* **441**, 1118 (2006).
 - [25] T. W. B. Kibble, *J. Phys. A* **9**, 1387 (1976); W. H. Zurek, *Nature (London)* **317**, 505 (1985).
 - [26] T. Frisch, Y. Pomeau, and S. Rica, *Phys. Rev. Lett.* **69**, 1644 (1992); B. Jackson, J. F. McCann, and C. S. Adams, *Phys. Rev. Lett.* **80**, 3903 (1998); T. Winiecki, J. F. McCann, and C. S. Adams, *Phys. Rev. Lett.* **82**, 5186 (1999).
 - [27] L. D. Landau, *J. Phys. USSR* **5**, 71 (1941).
 - [28] S. Inouye, S. Gupta, T. Rosenband, A. P. Chikkatur, A. Gorlitz, T. L. Gustavson, A. E. Leanhardt, D. E. Pritchard, and W. Ketterle, *Phys. Rev. Lett.* **87**, 080402 (2001); T. W. Neely, E. C. Samson, A. S. Bradley, M. J. Davis, and B. P. Anderson, *Phys. Rev. Lett.* **104**, 160401 (2010); W. J. Kwon, G. Moon, J. Choi, S. W. Seo, and Y. Shin, *Phys. Rev. A* **90**, 063627 (2014).
 - [29] M. Crescimanno, C. G. Koay, R. Peterson, and R. Walsworth, *Phys. Rev. A* **62**, 063612 (2000); W. J. Kwon, G. Moon, S. W. Seo, and Y. Shin, *Phys. Rev. A* **91**, 053615 (2015).
 - [30] L. Salasnich, A. Parola, and L. Reatto, *Phys. Rev. A* **65**, 043614 (2002).
 - [31] A. S. Rodrigues, P. G. Kevrekidis, R. Carretero-González, D. J. Frantzeskakis, P. Schmelcher, *Phys. Rev. A* **79**, 043603 (2009).
 - [32] J. J. Sakurai, *Modern Quantum Mechanics (Revised Edition)*, Addison Wesley, Reading, 1994, pp 158-174.
 - [33] S. Gautam and S. K. Adhikari, *Phys. Rev. A* **92**, 023616 (2015).
 - [34] S. Gautam and S. K. Adhikari, *Fractional-charge vortex in a spinor Bose-Einstein condensate*, arXiv:1601.01541.
 - [35] C. Huepe and M. E. Brachet, *Physica D* **140**, 126 (2000); N. G. Berloff and P. H. Roberts, *J. Phys. A: Math. Gen.* **33**, 4025 (2000); S. Rica, *Physica D* **148**, 221 (2001); C.-T. Pham, C. Nore, and M. E. Brachet, *Physica D* **210**, 203 (2005); F. Pinsker and N. G. Berloff, *Phys. Rev. A* **89**, 053605 (2014).
 - [36] S. Watabe, Y. Kato, and Y. Ohashi, *Phys. Rev. A* **84**, 013616 (2011).
 - [37] H. Pu and N. P. Bigelow, *Phys. Rev. Lett.* **80**, 1134 (1998); D. Gordon and C. M. Savage, *Phys. Rev. A* **58**, 1440 (1998).
 - [38] S. Gautam and S. K. Adhikari, *Phys. Rev. A* **90**, 043619 (2014); *Phys. Rev. A* **91**, 013624 (2015).
 - [39] P. Muruganandam and S. K. Adhikari, *Comput. Phys. Commun.* **180**, 1888 (2009); *J. Phys. B* **36**, 2501 (2003); D. Vudragovic, I. Vidanovic, A. Balaz, P. Muruganandam, and S. K. Adhikari, *Comput. Phys. Commun.* **183**, 2021 (2012); R. Kishor Kumar, L. E. Young-S., D. Vudragović, A. Balaz, P. Muruganandam, and S.K. Adhikari, *Comput. Phys. Commun.* **195**, 117 (2015).

- [40] S. Inouye, M. R. Andrews, J. Stenger, H.-J. Miesner, D. M. Stamper-Kurn, and W. Ketterle, *Nature* (London) **392**, 151 (1998); C. Chin, R. Grimm, P. Julienne, and E. Tiesinga, *Rev. Mod. Phys.* **82**, 1225 (2010).
- [41] V. Hakim, *Phys. Rev. E* **55**, 2835 (1997); N. Pavloff, *Phys. Rev. A* **66**, 013610 (2002).
- [42] A. C. Ji, W. M. Liu, J. L. Song, and F. Zhou, *Phys. Rev. Lett.* **101**, 010402 (2008); M. Eto, K. Kasamatsu, M. Nitta, H. Takeuchi, and M. Tsubota, *Phys. Rev. A* **83**, 063603 (2011); J. Lovegrove, M. O. Borgh, and J. Ruostekoski, *Phys. Rev. A* **86**, 013613 (2012).